Chapter 7
Contribution of Atmospheric Reactive Nitrogen to Ozone Pollution in China

Zhaozhong Feng, Wen Xu, and Bo Shang

Abstract This chapter illustrates mechanism of ozone (O_3) formation and summarizes the relationship between spatial-temporal patterns of NO_x emission and ground-level O_3 in China. High O_3 levels are observed in major Chinese metropolitan areas such as the Yangtze River Delta, Jing-Jin-Ji, and Pearl River region. Ambient O_3 concentrations in almost all monitor sites were above the threshold recommended for protecting plant growth. Thus, current O_3 levels have threatened the health and function of ecosystems. Impacts of ground-level O_3 on plants, including crops and tree species, are summarized based on the experimental results from open top chambers (OTCs) and free air ozone concentration elevation (O_3-FACE) facilities. Some recommendations for reduction of ground-level O_3 are presented in order to reduce its negative effects as concluding remarks of this chapter.

7.1 Introduction

Air pollution is a serious ecological issue in China's economically well-developed areas such as Yangtze River Delta, Beijing-Tianjin-Hebei, and Pearl River Delta regions (Wang et al. 2017). Air pollution in these areas not only deteriorates regional and urban air quality but also severely affects health of people and ecosystems (Zhang et al. 2016). Among six air pollutants (e.g., SO_2, $PM_{2.5}$, PM_{10}, NO_2, CO, and O_3) officially tracked by Chinese air quality monitoring platform (http://www.aqistudy.cn/), ground-level O_3 is the most phytotoxic air because it

Z. Feng (✉)
School of Applied Meteorology, Nanjing University of Information Science & Technology, Nanjing, China
e-mail: zhaozhong.feng@nuist.edu.cn

W. Xu
National Academy of Agriculture Green Development, China Agricultural University, Beijing, China

B. Shang
State Key Laboratory of Urban and Regional Ecology, Research Center for Eco-Environmental Sciences, Chinese Academy of Sciences, Beijing, China

X. Liu, E. Du (eds.), *Atmospheric Reactive Nitrogen in China*,
https://doi.org/10.1007/978-981-13-8514-8_7

causes severe plant damage and its high regional localized concentration (Feng et al. 2014, 2015a). Although in some areas O_3 level was decreased, especially in the USA and Europe (Cooper et al. 2015), ozone monitoring in China showed an increasing trend since the 1990s (Xu et al. 2008, 2016a; Wang et al. 2009), which became especially alarming in the last 5 years (2013–2016) (Lu et al. 2018; Zeng et al. 2019). Ozone pollution observed during summers in China is especially concerned. Particularly high O_3 levels were observed in multiple cities during summer 2017: 90th percentile of a daily maximum 8-h average (MDA8) O_3 level in 30 out of 74 major cities exceeded 200 μg/m^3. Air with such high O_3 concentrations corresponds to grade II according to the national air quality standards for residential areas (Lu et al. 2018). Ground-level O_3 in China strongly correlated with emissions of NO_x, which is a main contributor to O_3 formation (Wang et al. 2017). Literature results demonstrate 10% yield decrease for major food crops (such as potato, rice, wheat, soybeans, etc.) at O_3 concentrations in air equal to ~40 ppb in comparison with crop yields grown in O_3-free air (Feng and Kobayashi 2009). Survey in Beijing and its surroundings revealed 28 plant species or cultivars with typical O_3 symptoms (Feng et al. 2014). Thus, food security in China is being threatened or has already been severely affected by current high ground-level O_3 concentration. Without special measures and precautions, O_3 levels will continue to rise.

This chapter describes mechanism of ground-level O_3 formation and summarizes recent development based on the analysis and predictions of spatial-temporal distribution patterns of NO_x emission in China. It also discusses how ground-level O_3 affects the well-being of plants. Recommendations on adverse impact of ground-level O_3 pollution as well as way for its reduction and prevention are also illustrated.

7.2 Mechanism of O_3 Formation

Ozone forms in the atmosphere as a result of visible light-assisted reaction of various nitrogen oxides (formed in a $NO_x \leftrightarrow NO_2 + NO$ reaction) with volatile organic compounds (VOCs), methane (CH_4) and carbon monoxide (CO). Specifically, ozone formation is a combination reaction between molecular oxygen (O_2) and atomic oxygen ($O(^3P)$) (see Eq. 7.1). Atomic oxygen is obtained by O_2 decomposition upon its exposure to short-wavelength ultraviolet (UV) radiation with wavelengths below 240 nm. These reactions are responsible for producing and maintaining protective O_3 layer (Chapman 1930).

Troposphere does not have so much UV as other atmospheric layers; thus, NO_2 photolytic reaction occurring at wavelengths below 424 nm (as shown in Eq. 7.2) is a primary source of atomic $O(^3P)$, which becomes the major O_3-producing reaction.

In normal and well-balanced environment, freshly formed O_3 immediately reacts with NO to regenerate NO_2 (see Eq. 7.3). Thus, the whole reaction cycle shown by Eqs. 7.1, 7.2, and 7.3 yields no by- and/or final products when no other competing chemical species are involved:

$$O(^3P) + O_2 + M \rightarrow O_3 + M, \tag{7.1}$$

$$NO_2 + hv \rightarrow NO + O(^3P), \tag{7.2}$$

$$O_3 + NO \rightarrow NO_2 + O_2. \tag{7.3}$$

Nevertheless, molecules like HO_2 and RO_2 with very high oxidative activity are also present in the troposphere. These radicals can effectively transform NO to NO_2 (see Eqs. 7.4 and 7.5). Without enough NO present in the troposphere, not all freshly formed O_3 can react to decompose to O_2. Thus, ozone starts to accumulate in the troposphere. Reactions shown in Eqs. 7.2, 7.4, and 7.5 demonstrate "NO_x cycle," which produces O_3 without NO_x consumption (see Fig. 7.1).

Another significant chemical cycle affecting O_3 formation is "RO_x (RO_x = OH + HO_2 + RO_2) radical cycle." It constantly supplies HO_2 and RO_2 radicals that easily oxidize NO to NO_2. This cycle typically begins with OH-induced degradation of VOCs (see Eq. 7.6), which generates RO_2 radicals followed by their conversion to RO (see Eq. 7.5). Just formed RO easily reacts with O_2 yielding HO_2 (see Eq. 7.7), which then reacts with NO producing OH and NO_2 (see Eq. 7.4). Each

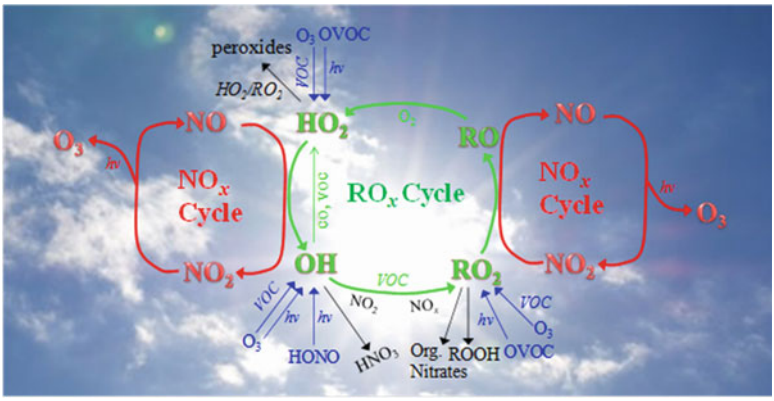

Fig. 7.1 Schematic of light-induced mechanism of O_3 formation as well as chemical and material balance relationship between RO_x- and NO_x-based cycles. Reactions and balances marked with red indicate NO_x cycle, green corresponds to RO_x cycle, blue shows radical initiation reactions, and black demonstrates termination processes. (This figure was adapted from Wang et al. (2017) with permission by Elsevier)

RO_x cycle consumes two NO molecules (and transforms them into NO_2), forms two O_3 molecules through a typical "NO_x cycle" (shown in Eqs. 7.1, 7.2, and 7.3), and recycles NO (from the NO_x cycle). Figure 7.1 demonstrates a schematic reflecting these two cycles (one chemical and one photochemical) occurring simultaneously.

$$HO_2 + NO \rightarrow OH + NO_2, \tag{7.4}$$

$$RO_2 + NO \rightarrow RO + NO_2, \tag{7.5}$$

$$OH + RH + O_2 \rightarrow RO_2 + H_2O, \tag{7.6}$$

$$RO + O_2 \rightarrow HO_2 + \text{carbonyls}. \tag{7.7}$$

Both NO_x and RO_x cycles terminate by their corresponding cross-reaction of RO_x and/or NO_x. At high NO_x concentration, termination by reactions with OH (Eq. 7.8) and RO_2 (Eq. 7.9) dominates. The products of these two reactions are organic nitrates (NO_z species) and nitric acid. When NO_x concentration is low, the main termination reactions are either recombination of hydroperoxyl radicals (see Eq. 7.10) or recombination of RO_2 and HO_2 radicals (Eq. 7.11), which yield hydrogen and organic peroxides. Thus, one can use NO_z concentration as well as H_2O_2/HNO_3 ratio to evaluate atmospheric conditions in terms of NO_x concentration (whether it is low or high). These ratios are also used as indicators showing which cycle formation of O_3 follows: VOC- or NO_x-based.

$$OH + NO_2 \rightarrow HNO_3, \tag{7.8}$$

$$RO_2 + NO_2 \leftrightarrow RO_2NO_2, \tag{7.9}$$

$$HO_2 + HO_2 \rightarrow H_2O_2 + O_2, \tag{7.10}$$

$$HO_2 + RO_2 \rightarrow RO_2H + O_2. \tag{7.11}$$

RO_x can also form from the closed-shell molecules. They participate in a standard RO_x cycle mentioned above and, thus, also play a substantial role in O_3 generation. In contaminated troposphere, RO_x radicals form as a result of O_3, HONO, and photolysis as well as from the O_3-induced cleavage of unsaturated VOCs. Contribution of radicals from different sources varies depending on geographical location (Xue et al. 2016). Relatively recent, new origins of atmospheric radicals as well as their precursors were discovered including previously unknown daytime and nighttime sources of HONO (Kleffmann 2007) and nitryl chloride ($ClNO_2$), respectively. Cl atom released from reaction formed in the dark $ClNO_2$ further reacts with VOCs. Products of this reaction benefit photochemical formation of O_3 by a gas-phase mechanism similar to a mechanism involving OH (e.g., Riedel et al. 2014):

$$RH + Cl + O_2 \rightarrow RO_2 + HCl. \tag{7.12}$$

All O_3 production routes have one common feature: ozone formation demonstrates a nonlinear relationship with concentration of its precursors (VOCs and/or NO_x). At low concentrations of NO_x/VOCs, NO_x cycle generates less O_3 produced

based on RO_x cycle. Thus, NO_x/VOC concentration becomes a limiting factor of O_3 generation. This situation is known as "NO_x-limited O_3 formation regime." In contrast, at high NO_x/VOC concentration, the limiting factors of O_3 production are intensity, speed, and rate of the RO_x-based cycle. This situation is often referred to as "VOC-limited." However, O_3 production through these cycles still remains somewhat complex as it is also influenced by VOC reactivity, NO_x/VOC ratios, photochemical aging, meteorological conditions, and biogenic emissions. Dominancy of NO_x- or RO_x-based cycles is also determined by the sources of reactive organic radicals (e.g., produced by photolysis of O_3, HCHO, etc.) as well as by traps of hydrogen radicals (see Eqs. 7.13, 7.14, 7.15, 7.16, and 7.17) (Sillman 1999):

Sources:

$$O_3 + h\nu \xrightarrow{H2O} H_2O \; 2OH, \tag{7.13}$$

$$HCHO + h\nu \xrightarrow{O2} O_2 \; HO_2 + CO. \tag{7.14}$$

Sinks:

$$HO_2 + HO_2 \rightarrow H_2O_2 + O_2, \tag{7.15}$$

$$RO_2 + HO_2 \rightarrow ROOH + O_2, \tag{7.16}$$

$$OH + NO_2 \rightarrow HNO_3. \tag{7.17}$$

Many urban areas are either VOC-sensitive or NO_x-saturated. Low levels of HO_x radicals removed by the reaction products between NO_2 and OH are responsible for decreased O_3 concentration in urban areas. Additionally, ground-level O_3 concentration can be reduced because of so-called "NO_x titration": in areas with substantial NO concentrations in the atmosphere (e.g. from car exhausts), O_3 reacts with NO.

Several recent studies (Tang et al. 2012; Tie et al. 2013; Xue et al. 2014) explored O_3 formation pathways in China. It is a very important step toward the development of scientific approaches toward regulation and control of ground-level O_3 levels. Thus, it was reported that VOC-based formation of O_3 dominates in the Pearl River region and in Central Eastern China. At the same time, in the summer, O_3 formation in areas with plain and mountain landscapes located in Northern China was sensitive to both VOC and NO_x, respectively (Tang et al. 2012). In cities and surrounding areas of Yangtze River Delta and North China Plain as well as PRD regions, O_3 formation is VOC-limited (Tie et al. 2013; Xue et al. 2014). In other words, NO_x present in Chinese cities induces "titration effect" mentioned above. Unfortunately, this kind of scientific research information is still limited, which slows down full and detailed understanding of processes of ground-level O_3 formation. Research of O_3-VOC-NO_x chemistry in atmosphere over China requires further improvement, which can be achieved by thorough data collection, experimental observations, and theoretical simulations, all of which are crucial for development of effective industrial and governmental policies for ground-level O_3 pollution control.

7.3 Spatial-Temporal Pattern of NO_x Emission Over China

Nitrogen dioxide (NO_2) and nitrogen oxide (NO), often combined under a general name nitrogen oxides (NO_x), are present in the atmosphere as gas in trace amounts and have short life period. Yet, they are very active participants in O_3 formation (Seinfeld and Pandis 2006). Anthropogenic activities, especially usage and consumption of fossil fuel, are the major contributors to NO_x in the atmosphere especially at high concentrations of NO_x near or around densely populated urban and suburban/rural industrial areas as well as around power plants.

China is one of the major contributors to atmospheric NO_x pollution in the world as it contributes to ~18% of the global NO_x emissions (EDGAR 4.2, EC-JRC/PBL 2011). China's NO_x release increased 1.5 times from 1980 to 1995 as Chinese GDP was increasing by 10% annually during the same time frame (Klimont et al. 2009). Because of Asian economy crisis, NO_x emissions started to decline in 1996 and continued to decrease till 2000. Utilization of coal relative to the total energy consumption decreased from 77% to 71%, which was reflected in NO_x emission reduction during the 1996–2000 period (Hao et al. 2002; NBS 2010). After the economy started to recover in 2000, NO_x emission quickly reached pre-crisis level and even doubled it (Fig. 7.2) as utilization of coal increased twofold in the 2001–2008 time period (NBS 2010). Between 1995 and 2005, NO_x emissions increased by 6.3% annually (Zhang et al. 2007). Nevertheless, since strict pollution-control preventive and technical measures were implemented in 2011, fast growth of NO_x concentration in the atmosphere slowed down and eventually reversed (see Fig. 2.1 in Chap. 2 and Fig. 5.6 in Chap. 5).

Chinese government went even further and implemented new regulations to decrease emissions and to improve air quality. The goal was to cut national total

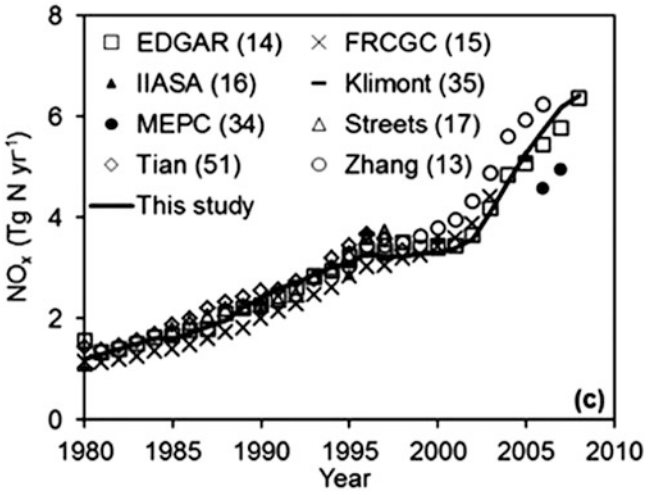

Fig. 7.2 NO_x emission trend during 1980–2010 period. (This figure was adapted from Gu et al. (2012) with permission by American Chemical Society)

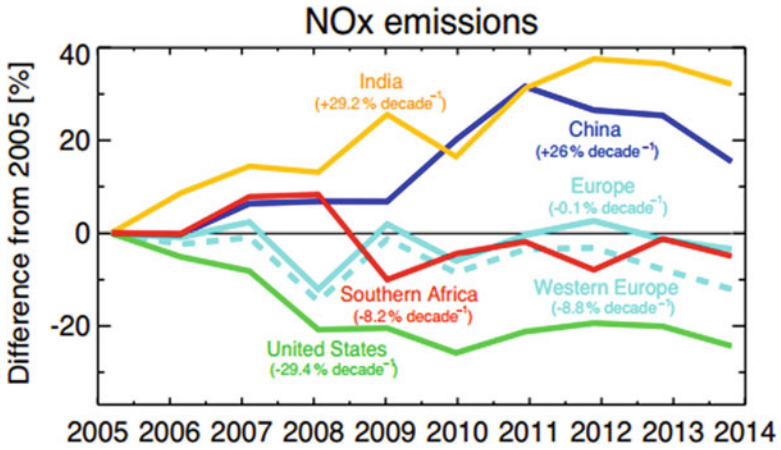

Fig. 7.3 Annual NO_x emissions detected in the atmosphere during 2005–2014 monitoring period for India (yellow curve), China (dark blue curve), Europe (cyan curve), Western Europe (cyan dashed line), Southern Africa (red), and the USA (green). Emission values are reported relative to emissions in each country in 2005. (This figure was adapted from Miyazaki et al. (2017) under the Creative Commons Attribution License)

NO_x emissions by 10% in 2015 relative to emissions in 2011. Several studies showed that OMI NO_2 levels increased from 2005 to 2011 followed by a slight decrease (Krotkov et al. 2016; Duncan et al. 2016). Reduction of NO_x emissions originating from China after 2011–2012 was confirmed based on satellite data by various researches (e.g., Miyazaki et al. 2017; Souri et al. 2017; Van der A et al. 2017). Latest estimations showed that NO_x emission decreased by ~20% during the 2010–2017 period (see Fig. 2.1 in Chap. 2). However, taking a 10-year period covering years from 2005 to 2014, an increasing trend was demonstrated in the amount of NO_x emissions in China despite significant year-to-year variations. According to Miyazaki et al. (2017), linear fitting of the NO_x emission data over the 10-year period revealed a slope equivalent to 26% increase (see Fig. 7.3).

Especially substantial NO_x emissions were detected in large cities such as Wuhan, Nanjing, Tianjin, and Chengdu, in which ground-level concentrations of NO_x increased by 42%, 35%, 35%, and 56% per decade, respectively. An overall increase in Eastern China was also detected (see Fig. 7.4). A significant increase in NO_x concentration occurred in Western China, especially its Northern regions (~88 to 110°E, 37–48°N): NO_x concentration in air in these regions increased by 50–110% per decade. In spite of a general large and positive trend, the three largest Chinese cities (Beijing, Shanghai, and Guangzhou) demonstrated either small reduction or a small 10-year increase in NO_x emissions during 2005–2014: −0.6%, −6.2%, and 4.5%, respectively. The same trends were observed specifically for NO_2 emissions (Wang et al. 2015).

NO_x emissions also demonstrate spatial variability in China (see Fig. 7.5a). In 2004, regions with highest NO_x emissions were mostly located on the East Coast: from Southern Yangtze Delta region around Shanghai to North of Beijing (Zhang

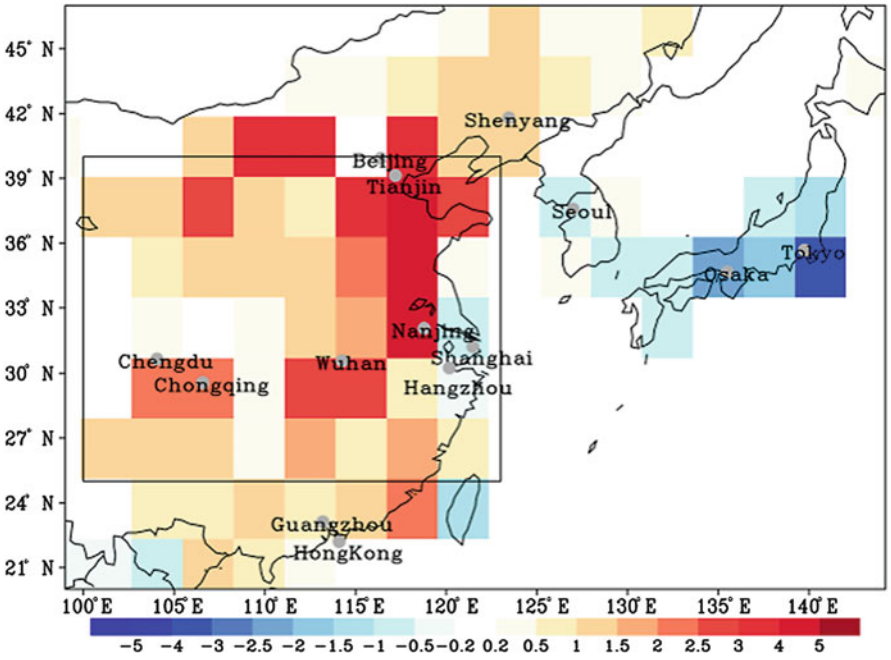

Fig. 7.4 NO_x emissions (in 10^{-11} kg m^{-2} s^{-1} per decade) during 2005–2014 period in different countries and regions of Asia (upper left panel). (This figure was adapted from Miyazaki et al. (2017) under the Creative Commons Attribution License)

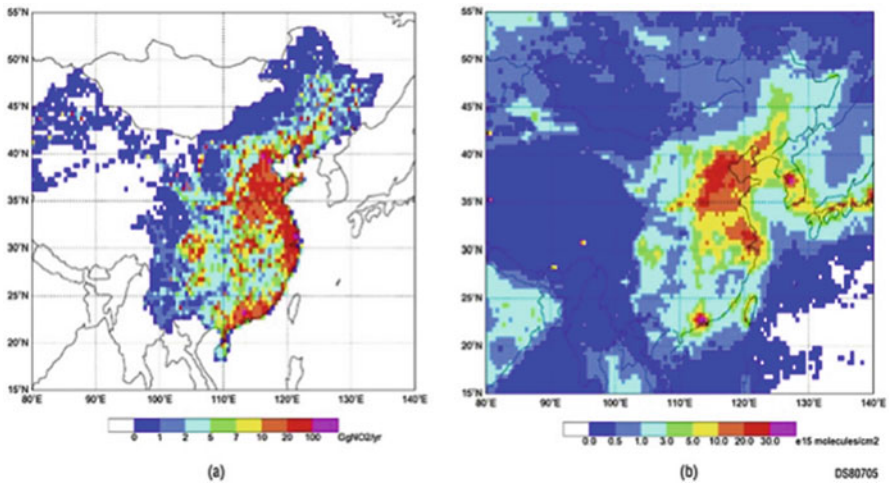

Fig. 7.5 Spatial distribution of (**a**) NO_x emission and (**b**) SCIAMACHY tropospheric NO_2 vertical columns in 2004. (This figure was adapted from Zhang et al. (2007) with permission by John Wiley and Sons)

et al. 2007). Pearl River Delta (PRD) region of Hong Kong and Guangzhou as well as Sichuan Basin also exhibited high NO_x emissions. Regional distribution of NO_x emissions shown in Fig. 7.5 corresponds very well to the tropospheric NO_2 columns derived from SCIAMACHY measurements in 2004 (Fig. 7.5b): columns with high NO_2 concentration were spread across East China and PRD regions in a similar way as spatial distribution of NO_x shown in Fig. 7.5a.

Between 2007 and 2015, provinces with the highest NO_x emission in China were Anhui, Shandong, Henan, Hebei, Jiangsu, Guangdong, Zhejiang, Shanxi, Sichuan, and Hubei. Combined, emissions from these provinces accounted for 65% of all NO_x emissions in China (van der et al. 2017).

7.4 Spatial-Temporal Pattern of Ground-Level O_3 in China

Fast industrial and urban developments in China led to higher amounts of O_3 precursors (mainly NO_x and VOCs) participating and assisting O_3 formation, which is the reason for high-increasing rate in ground-level O_3 concentrations in China (Wang and Mauzerall 2004; Feng et al. 2015a).

Ground-level O_3 concentration in China as well as their variations (both spatial and temporal) was thoroughly analyzed. Li et al. (2017a) collected data on ground-level O_3 levels at 187 cities from January 2015 to November 2016. Publication and official release of this data revealed significant spatial variation of O_3 in China. Averaged O_3 concentrations ranged from 50.6 ppb (in Nanchong) to 64.1 ppb (in Yixing, which is an industrial city in the Yangtze River Delta). High O_3 levels were also detected in major Chinese metropolitan areas located in Jing-Jin-Ji and in deltas of the Yangtze and Pearl Rivers (see Fig. 7.6). Rapid growth and development of different industries, including transportation and urban branches, in these cities as well as around them is the major driving force responsible for the O_3 pollution.

Average O_3 concentration over China increased from 46.1 ± 8.8 ppb in 2014 to 51.9 ± 7.8 ppb in 2016 (see Fig. 7.6). Significant O_3 level increase was observed in the Yangtze River Delta, North China Plain, and Inner Mongolian and even Southeastern Tibetan Plateau. However, levels of NO_2 demonstrated a slight decreasing trend (Li et al. 2017a). We already mentioned above that O_3 increase in different regions is caused by different factors. Three major factors can be described as follows. (1) Industrialized areas demonstrate increased ground-level O_3 concentration because of high VOC emissions (Yuan et al. 2013), which, in turn, leads to more rapid formation of O_3. (2) In North China Plain, lowered NO_x emission inhibits titration reaction between NO and O_3, which also results in high O_3 concentrations (Xu et al. 2016b). (3) High O_3 levels in Tibet Plateau can be explained by strong stratosphere-troposphere exchange processes because of the narrow troposphere layer in Tibetan Plateau (Skerlak et al. 2014).

Several studies predicted future changes in ground-level O_3 concentrations in China. Zhu and Liao (2016) used high-resolution nested grid version of the GEOS-Chem model to simulate changes in ground-level O_3 concentrations for the

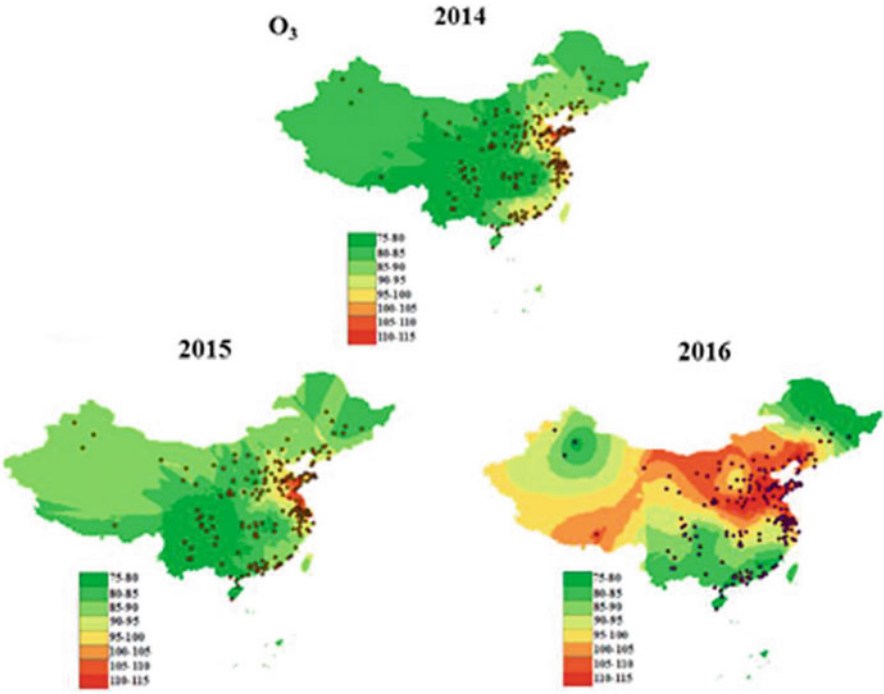

Fig. 7.6 Variation of ground-level O_3 during 2014–2016 period in China. (This figure was adapted from Li et al. (2017a) with permission by Elsevier)

2000–2050 period in response to the changes in anthropogenic emissions under the RCP2.6, RCP4.5, RCP6.0, and RCP8.5. Annual ground-level O_3 concentration predicted from the year 2010 to 2050 for every decade relative to 2000 values under the four RCPs are shown in Fig. 7.7. Under these four RCPs, predicted changes in annual mean ground-level O_3 levels showed different trends. RCP8.5 predicted the worst scenario for 2020–2030, and RCP6.0 showed the worst situation over 2040–2050.

Typically, O_3 levels are also significantly higher in the summer than in the winter (Fig. 7.8). Formation rate of O_3 depends on solar radiation intensity, and thus shorter light days and insufficient amount of sunlight inhibit O_3 formation in winter (Li et al. 2017a). During spring and summer, higher temperatures and stronger solar radiation helps to generate many OH radicals, which react with VOC and further enhance rate of O_3 formation. Furthermore, stratosphere-troposphere exchange processes in springs and summers also lead to increased O_3 levels (Ou et al. 2015).

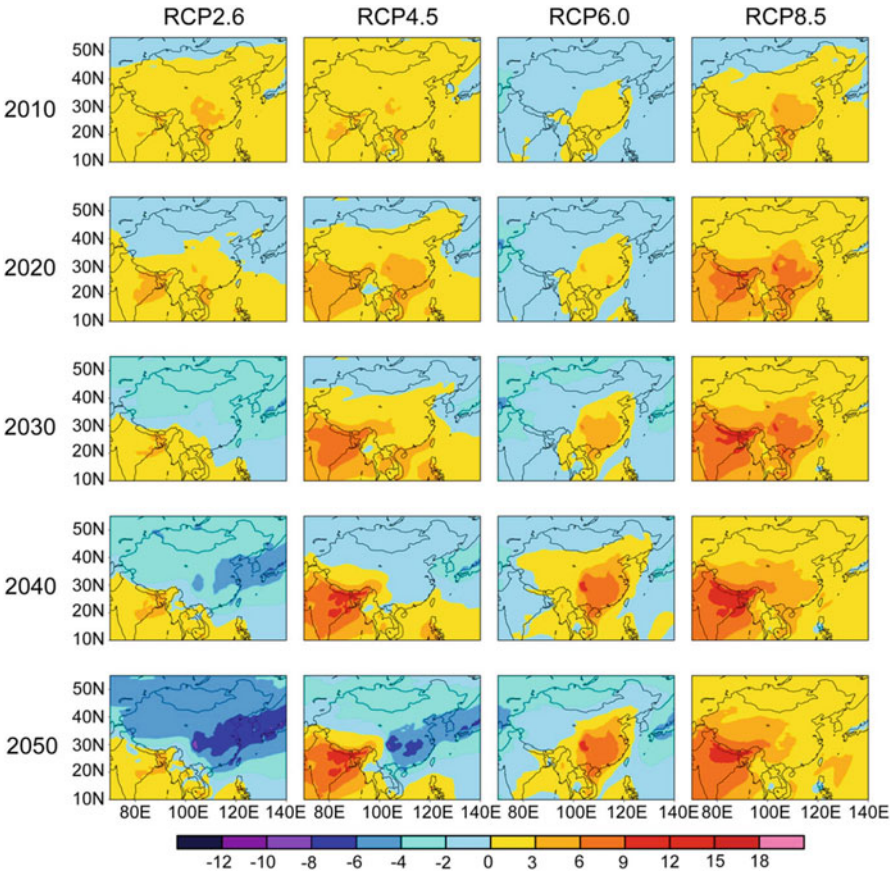

Fig. 7.7 Predicted (for years 2010–2050) average annual values of ground-level O_3 concentrations (ppb) shown relative to the values of 2000 year under the four RCPs. (This figure was adapted from Zhu and Liao (2016) with permission by Elsevier)

7.5 Impact of Ground-Level O_3 on Plants

High O_3 concentrations cause severe plant damage through a three-step process: exposure, uptake, and bio-effect. Ozone mainly enters plants through leaf stomata, and the entry of O_3 could be controlled by stomata. After O_3 molecular enters a substomatal cavity, it quickly binds with molecules of the adjacent cell walls or of the outer cell membrane. The intercellular O_3 concertation is almost zero because of very quick chemical reactions occurring in that part of a plant. Nevertheless, the

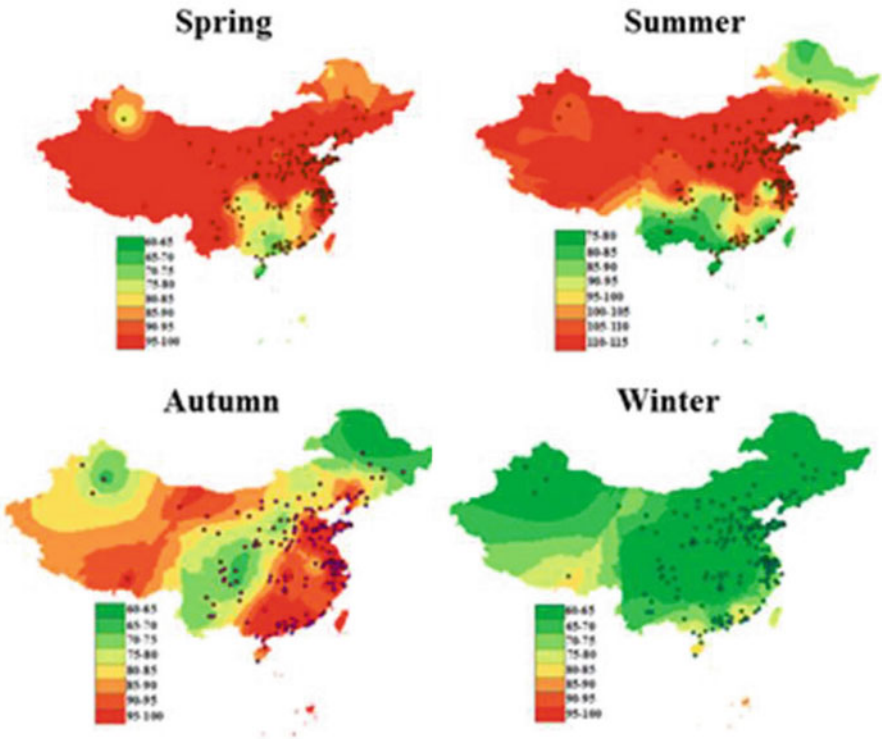

Fig. 7.8 Seasonal variation of ground-level O_3 in China. (This figure was adapted from Li et al. (2017a) with permission by Elsevier)

reactive oxygen species (ROS) or biomolecule oxidation products formed as a result of O_3 interaction with cellular redox systems originate or support reactions in physiological tissues (Tausz et al. 2007). Schematics of O_3 effects on plants are shown in Fig. 7.9 (Renaut et al. 2009). Ground-level O_3 caused visible leaf injury, which also reduced photosynthesis and inhibited growth and yield. High O_3 level also changes how plants deal with diseases and pests (Krupa et al. 2000).

High O_3 levels could affect plant leaves, and the visible O_3 symptoms of plant leaves could be used to visually quickly assess and predict O_3 pollution in the field conditions (Hayes et al. 2007). Feng et al. (2014) examined clearly visible plant injuries in July and August of 2013 in parks, forests, and agricultural regions of Beijing, China. The visible injury was detected in many areas and in 28 different plant species or cultivars. Ozone symptoms were observed more frequently in rural and mountain areas of Northern Beijing, which are located downwind from the city. Less leaves damage was observed in city gardens. Injuries to crop-bearing plants were detected most frequently for genera *Phaseolus*, *Canavalia*, and *Vigna* beans

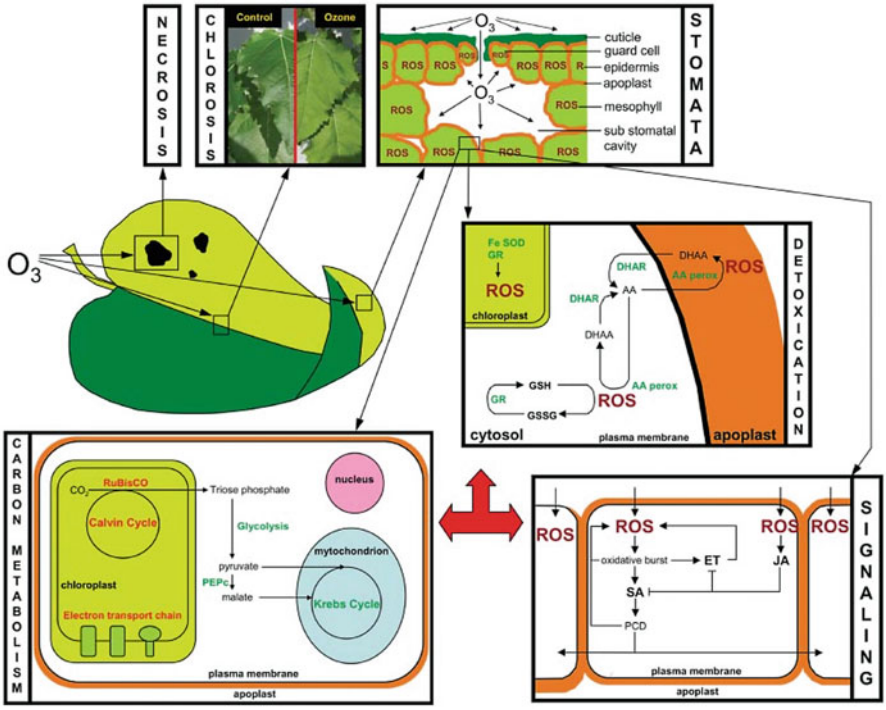

Fig. 7.9 Schematics of main physiological processes for the effects of O_3 on plant leaves. Exposure to high O_3 levels leads to leaves chlorosis and necrosis. Ozone molecules diffuse through the stomata inside the leaves. Ozone enters mainly through the leaves' stomata. The major O_3 detoxification process incudes ascorbate, glutathione, and SOD. Ozone activates signaling processes based on ethylene, salicylic acid, and jasmonic acids. Different pathways initiate different responses: jasmonic acid pathway inhibits routes based on ethylene and salicylic acid. Photosynthesis rate slows down at both photochemical and biochemical levels during exposure. At the same time, respiration is enhanced including anaplerotic pathway involving PEPc. The following abbreviations were used: AA, SA, and JA stand for ascorbic, salicylic, and jasmonic acids; AAperox indicates ascorbic acid peroxidase; DHAA means dehydroascorbic acid; ET stands for ethylene; GR represents glutathione reductase; GSH and GSSG indicate reduced and oxidized glutathione, respectively; PCD stands for programmed cell death; PEPc stands for phosphoenolpyruvate carboxylase; ROS stands for reactive oxygen species; RuBisCO stands for ribulose-1,5-bisphosphate carboxylase/oxygenase; SOD stands for superoxide dismutase. (This figure was adapted from Renaut et al. (2009) with permission by Elsevier)

and still observed but less often for watermelon, grapevines, and gourds. Several native trees, such as pines, ailanthus, and ash trees, also showed symptoms. Rose of Sharon, black locust, and Japanese morning glory were among the injured ornamental plants. Examples of O_3 symptoms are shown in Fig. 7.10 for some of the plants mentioned above (Feng et al. 2014).

Fig. 7.10 Ozone symptoms in plants native to Beijing area of China: *Ailanthus altissima* (1), *Ampelopsis humulifolia* (2), *Fraxinus rhynchophylla* (3), *Pinus bungeana* (4). Ornamental plants: *Robinia pseudoacacia* (5) and *Hibiscus syriacus* (6). Crops: *Canavalia gladiate* (7), *Vigna unguiculata* var. heterophylla (8), *Benincasa pruriens* (9), *Luffa cylindrica* (10), *Citrullus lanatus* (11), and *Vitis vinifera* (12). (This figure was adapted from Feng et al. (2014) with permission by Elsevier)

Current O_3 levels in China are high enough to cause chronic changes in trees such as reduced photosynthesis, decreased productivity, and accelerated leaf senescence. Such severe damage should not be unnoticed because forests and trees are the most important carbon sinks (Wittig et al. 2009).

China is one of the world's most forest-deficient countries: forests cover only 22% of the total land area, which is significantly less than a 30% global average (Fang et al. 2014). Capacity and strength of carbon sink by boreal forests at midlatitudes of the northern hemisphere are significantly reduced because of

ground-level O_3 pollution. Li et al. (2017b) quantitatively analyzed data from Chinese studies on temperate and subtropical regions to determine how elevated O_3 concentrations affect vegetation growth, biomass, and functional leaf traits of different types of woody plants. Their results indicated that if averaged O_3 level is equal to 116 ppb, total biomass of woody plants would decrease by 14% comparing with O_3 levels equal to ~21 ppb. Effect of elevated O_3 concentration on biomass, growth, leaf characteristics, photosynthetic pigments, gas exchange, chlorophyll fluorescence, and antioxidant parameters for all kinds of trees in China are shown in Fig. 7.11 (Li et al. 2017b).

In fact, high O_3 level is one of the most damaging pollutants that severely damage economic and biological aspects of crop-bearing plants (Feng et al. 2011). Current ground-level O_3 concentration significantly decreased wheat growth as well as its quality and yield according to the meta-analysis, which are shown in Fig. 7.12 (Pleijel et al. 2018). Feng et al. (2015b) reviewed data on how elevated O_3 levels affect food crops in China and also demonstrated significant reduction in wheat yield. Based on exposure concentration and stomatal O_3 flux-response relationships obtained by O_3-FACE experimental data, they predicted that if O_3 level continues to increase, wheat crops will produce less yield by 6.4%–14.9% and 14.8%–23.0%, respectively. Thus, if O_3 level continues rising, food security in China might be severely compromised. Without certain regulations, precautions, and measures, ground-level O_3 levels will continue to rise and to damage forests and crops.

7.6 Mitigation Measures of Ozone Pollution

Ozone causes so much damage to vegetation, and finding a solution on how to control O_3 pollution is a worldwide concern. Yet, there is no a single solution to this issue. Below are several policy recommendations and mitigation measures, which should help to decrease O_3 impacts and to mitigate risks associated with high O_3 levels:

1. Strict control of emissions containing potential agents participating in O_3 formation cycle

Strict laws on O_3-related precursor (such as VOCs and NO_x) emissions are required. Currently, majority of these chemicals are from automotive exhausts. One solution is to impose a Euro standard V for all vehicle exhaust gases throughout China by no later than 2020. Another solution is to decrease personal use of cars and to encourage usage of public transportation in major and overpopulated areas. One way to regulate this is to increase gasoline price and parking fees (Feng et al. 2015a, b).

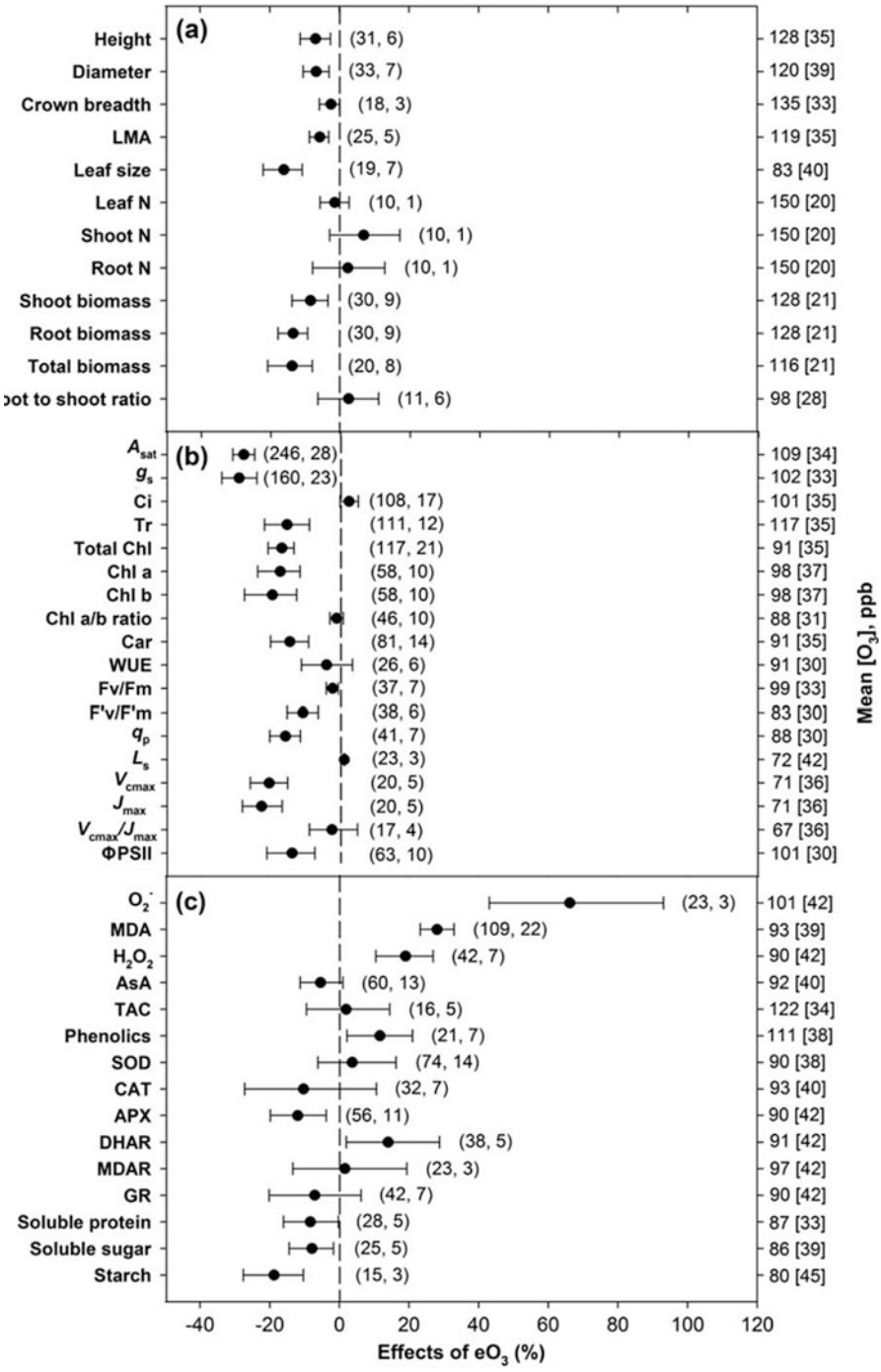

Fig. 7.11 Effect of elevated O_3 concentration (eO_3) on (**a**) biomass, growth and leaf characteristics, (**b**) photosynthetic pigments, gas exchange, chlorophyll fluorescence, and (**c**) antioxidant parameters of all trees. Data symbols represent percentage of the average value obtained at elevated O_3 concentration relative to the average value obtained at control O_3 concentration. Error bars reflect

2. Planting O_3-resistant plants

Different plants have different sensitivity under high O_3 levels. Thus, O_3-resistant genotypes can be selected, reproduced, and/or genetically modified by adding O_3-resistant genes. Such genes were already discovered for rice and soybean (Frei et al. 2010; Gillespie et al. 2011). Additionally, there are a large number of studies on the sensitivity of plants to O_3. For example, Feng et al. (2018) demonstrated that a lot of O_3 sensitivity variation for different woody plants can be explained by interspecific variation in LMA. Thus, ozone-tolerant plants can be chosen based on these rules and planted in certain O_3-rich areas to maintain their vegetation and to reduce the damage under high O_3 levels.

3. Ozone uptake through plants

Typically, ozone enters a plant through its leaf stomata, after which plants absorb O_3 and reduced O_3 content in the ambient air. This ability of plants to purify air is an important property that can be used at urban, ecological, and environmental planning and landscaping. However, plant-derived BVOCs can also participate in O_3 formation. Thus, high O_3 uptake and low-BVOC emission plants should be considered to efficiently control O_3 levels.

4. Application of chemical protective agents at specific phenological stages

Ozone-caused damage to plants could be decreased or prevented by application of antioxidants (e.g., glutathione, ascorbic acid, antiozonant ethylenediurea (EDU), etc.) (Feng et al. 2010; Manning et al. 2011). Such chemical agents are indeed widely used in the USA and many European countries to protect crops against high ambient O_3. However, the toxicity of EDU in the food chain is yet to be extensively tested, and the phytotoxicity can happen at high doses of EDU (Manning et al. 2011). Thus, most effective approach is to apply such agents at specific phenological stages, such as grain filling in both soybeans and wheat, during rice tillering, etc. It is necessary to apply these chemical protective agents to protect crops from production in high O_3 concentration areas. However, further testing of EDU toxicity and its impact on different crops are required through the field experiment.

Fig. 7.11 (continued) 95% bootstrapped confidence intervals. Number of measurements and papers are shown in parentheses, whereas mean elevated O_3 concentration and control O_3 concentration in square brackets are given along the y-axis. The following abbreviations were used to represent parameters studied: *φPSII* effective quantum yield of photosystem II, *APX* ascorbate peroxidase, *AsA* ascorbic acid, *Car* carotenoid, *CAT* catalase, *DHAR* dehydroascorbate reductase, *GR* glutathione reductase, *LMA* leaf mass per area, *MDA* malondialdehyde, *MDAR* monoascorbate reductase, *SOD* superoxide dismutase activity, *TAC* total antioxidant capacity, *WUE* water-use efficiency. (This figure was adapted from Li et al. (2017b) with permission by John Wiley and Sons)

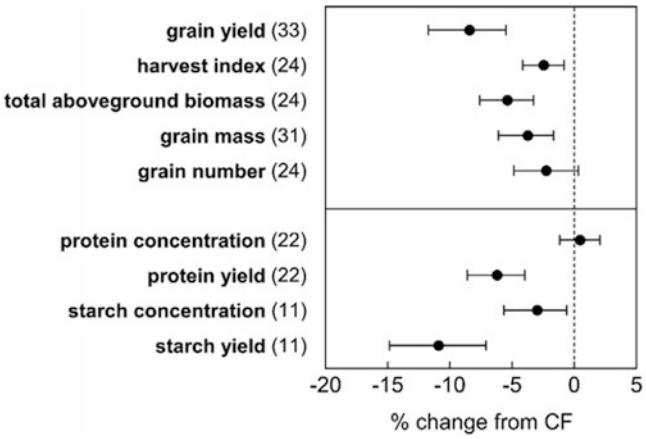

Fig. 7.12 Meta-analysis of the effect of non-filtered air (NF) vs. charcoal-filtered air (CF) for agronomically important wheat variables. Values in brackets indicate number of NF-CF comparisons for each variable. Error bars are 95% confidence intervals. (This figure was adapted from Pleijel et al. (2018) with permission by Elsevier)

References

Chapman S (1930) A theory of upper-atmospheric ozone. Edward Stanford, London

Cooper OR, Langford AO, Parrish DD et al (2015) Atmosphere. Challenges of a lowered U.S. ozone standard. Science 348:1096–1097

Duncan BN, Lamsal LN, Thompson AM et al (2016) A space-based, high-resolution view of notable changes in urban NO_x pollution around the world (2005–2014). J Geophys Res 121:976–996

Fang JY, Guo ZD, Hu HF et al (2014) Forest biomass carbon sinks in East Asia, with special reference to the relative contributions of forest expansion and forest growth. Glob Chang Biol 20:2019–2030

Feng ZZ, Kobayashi K (2009) Assessing the impacts of current and future concentrations of surface ozone on crop yield with meta-analysis. Atmos Environ 43:1510–1519

Feng ZZ, Wang SG, Szantoi Z et al (2010) Protection of plants from ambient ozone by applications of ethylenediurea (EDU): a meta-analytic review. Environ Pollut 158:3236–3242

Feng ZZ, Pan J, Kobayashi et al (2011) Differential responses in two varieties of winter wheat to elevated ozone concentration under fully open-air field conditions. Glob Chang Biol 17:580–591

Feng ZZ, Sun JS, Wan WX et al (2014) Evidence of widespread ozone-induced visible injury on plants in Beijing, China. Environ Pollut 193:296–301

Feng ZZ, Hu EZ, Wang XK et al (2015a) Ground-level O_3 pollution and its impacts on food crops in China: a review. Environ Pollut 199:42–48

Feng ZZ, Liu XJ, Zhang FS (2015b) Air pollution affects food security in China: taking ozone as an example. Front Agr Sci Eng 2:152–158

Feng ZZ, Büker P, Pleijel H et al (2018) A unifying explanation for variation in ozone sensitivity among woody plants. Glob Chang Biol 24:78–84

Frei M, Tanaka JP, Chen CP et al (2010) Mechanisms of ozone tolerance in rice: characterization of two QTLs affecting leaf bronzing by gene expression profiling and biochemical analyses. J Exp Bot 61:1405–1417

Gillespie KM, Rogers A, Ainsworth EA (2011) Growth at elevated ozone or elevated carbon dioxide concentration alters antioxidant capacity and response to acute oxidative stress in soybean (*Glycine max*). J Exp Bot 62:2667–2678

Gu BJ, Ge Y, Ren Y et al (2012) Atmospheric reactive nitrogen in China: sources, recent trends, and damage costs. Environ Sci Technol 46:9240–9247

Hao J, Tian H, Lu Y (2002) Emission inventories of NO_x from commercial energy consumption in China, 1995–1998. Environ Sci Technol 36:552–560

Hayes F, Mills G, Harmens H et al (2007) Evidence of widespread ozone damage to vegetation in Europe (1990–2006). Programme Coordination Centre for the ICP Vegetation, Centre for Ecology and Hydrology, Bangor. ISBN 978-0-9557672-1-0

Kleffmann J (2007) Daytime sources of nitrous acid (HONO) in the atmospheric boundary layer. Chem Phys Chem 8:1137–1144

Klimont Z, Cofala J, Xing J et al (2009) Projections of SO_2, NO_x and carbonaceous aerosols emissions in Asia. Tellus Ser B 61:602–617

Krotkov NA, McLinden CA, Li C et al (2016) Aura OMI observations of regional SO_2 and NO_2 pollution changes from 2005 to 2015. Atmos Chem Phys 16:4605–4629

Krupa S, McGrath MT, Andersen CP et al (2000) Ambient ozone and plant health. Plant Dis 85:4–12

Li R, Cui L, Li J et al (2017a) Spatial and temporal variation of particulate matter and gaseous pollutants in China during 2014–2016. Atmos Environ 161:235–246

Li P, Feng ZZ, Catalayud V et al (2017b) A meta-analysis on growth, physiological, and biochemical responses of woody species to ground-level ozone highlights the role of plant functional types. Plant Cell Environ 40:2369–2380

Lu X, Hong J, Zhang L et al (2018) Severe surface ozone pollution in China: a global perspective. Environ Sci Tech Lett 5:487–494

Manning WJ, Paoletti E, Sandermann H Jr et al (2011) Ethylenediurea (EDU): a research tool for assessment and verification of the effects of ground level ozone on plants under natural conditions. Environ Pollut 159:3283–3293

Miyazaki K, Eskes H, Sudo K et al (2017) Decadal changes in global surface NO_x emissions from multi-constituent satellite data assimilation. Atmos Chem Phys 17:807–837

National Bureau of Statistics (NBS) (2010) China statistical yearbook. National Bureau of Statistics of China Press, Beijing, pp 1981–2009

Ou J, Zheng J, Li R et al (2015) Speciated OVOC and VOC emission inventories and their implications for reactivity-based ozone control strategy in the Pearl River Delta region. China Sci Total Environ 530:393–402

Pleijel H, Broberg M, Uddling J et al (2018) Current surface ozone concentrations significantly decrease wheat growth, yield and quality. Sci Total Environ 613–614:687–692

Renaut J, Bohler S, Hausman JF (2009) The impact of atmospheric composition on plants: a case study of ozone and poplar. Mass Spectrom Rev 28:495–516

Riedel TP, Wolfe GM, Danas KT et al (2014) A MCM modeling study of nitryl chloride ($ClNO_2$) impacts on oxidation, ozone production and nitrogen oxide partitioning in polluted continental outflow. Atmos Chem Phys 14:3789–3800

Seinfeld JH, Pandis SN (2006) Atmospheric chemistry and physics: from air pollution to climate change. Wiley, New York, pp 204–275

Sillman S (1999) The relation between ozone, NO_x and hydrocarbons in urban and polluted rural environments. Atmos Environ 33:1821–1845

Skerlak B, Sprenger M, Pfahl S et al (2014) Rapid exchange between the stratosphere and the planetary boundary layer over the Tibetan Plateau, EGU General Assembly Conference Abstracts, p 9903

Souri AH, Choi Y, Jeon W et al (2017) Remote sensing evidence of decadal changes in major tropospheric ozone precursors over East Asia. J Geophys Res 122:2474–2492

Tang G, Wang Y, Li X et al (2012) Spatial-temporal variations in surface ozone in Northern China as observed during 2009-2010 and possible implications for future air quality control strategies. Atmos Chem Phys 12:2757–2776

Tausz M, Grulke NE, Wieser G (2007) Defense and avoidance of ozone under global change. Environ Pollut 147:525–531

Tie X, Geng F, Guenther A et al (2013) Megacity impacts on regional ozone formation: observations and WRF-Chem modeling for the MIRAGE-Shanghai field campaign. Atmos Chem Phys 13:5655–5669

Wang XP, Mauzerall DL (2004) Characterizing distributions of surface ozone and its impact on grain production in China, Japan and South Korea: 1990 and 2020. Atmos Environ 38:4383–4402

Wang T, Wei X, Ding A et al (2009) Increasing surface ozone concentrations in the background atmosphere of Southern China, 1994–2007. Atmos Chem Phys 9:6217–6227

Wang JM, Jeong CH, Zimmerman N et al (2015) Plume-based analysis of vehicle fleet air pollutant emissions and the contribution from high emitters. Atmos Meas Tech 8:3263–3275

Wang T, Xue L, Brimblecombe P et al (2017) Ozone pollution in China: a review of concentrations, meteorological influences, chemical precursors, and effects. Sci Total Environ 575:1582–1596

Wittig VE, Ainsworth EA, Naidu SL et al (2009) Quantifying the impact of current and future tropospheric ozone on tree biomass, growth, physiology and biochemistry: a quantitative meta-analysis. Glob Chang Biol 15:396–424

Xu W, Lin W, Wang T et al (2008) Long-term trend of surface ozone at a regional background station in eastern China 1991–2006: enhanced variability. Atmos Chem Phys 8:2595–2607

Xu W, Lin W, Xu X et al (2016a) Long-term trends of surface ozone and its influencing factors at the Mt Waliguan GAW station, China – part 1: overall trends and characteristics. Atmos Chem Phys 16:6191–6205

Xu RG, Tang GQ, Wang YS et al (2016b) Analysis of a long-term measurement of air pollutants (2007–2011) in North China Plain (NCP); impact of emission reduction during the Beijing Olympic games. Chemosphere 159:647–658

Xue LK, Wang T, Gao J et al (2014) Ground-level ozone in four Chinese cities: precursors, regional transport and heterogeneous processes. Atmos Chem Phys 14:13175–13188

Xue L, Gu R, Wang T et al (2016) Oxidative capacity and radical chemistry in the polluted atmosphere of Hong Kong and Pearl River Delta region: analysis of a severe photochemical smog episode. Atmos Chem Phys 16:9891–9903

Yuan B, Hu W, Shao M et al (2013) VOC emissions, evolutions and contributions to SOA formation at a receptor site in eastern China. Atmos Chem Phys 13:8815–8832

Zeng YY, Cao YF, Qiao X, Seyler BC, Tang Y (2019) Air pollution reduction in China: recent success but great challenge for the future. Sci Total Environ 663:329–337

Zhang Q, Streets DG, He K et al (2007) NO_x emission trends for China, 1995–2004: the view from the ground and the view from space. J Geophys Res-Atmos 112:D22306

Zhang H, Wang S, Hao J et al (2016) Air pollution and control action in Beijing. J Clean Prod 112:1519–1527

Zhu J, Liao H (2016) Future ozone air quality and radiative forcing over China owing to future changes in emissions under the representative concentration pathways. J Geophys Res 121:1978–2001

van der ARJ, Mijling B, Ding J et al (2017) Cleaning up the air: effectiveness of air quality policy for SO_2 and NO_x emissions in China. Atmos Chem Phys 17:1775–1789